Article

New Insights for Improving Low-Rank Coal Flotation Performance via Tetrahydrofurfuryl Ester Collectors

Xin Wang [1,2], Rui Ding [1,2], Xinyu Cui [1,2], Yonghong Qin [1,2], Gan Cheng [1,2], George Abaka-Wood [3] and Enze Li [1,2,*]

[1] State Environmental Protection Key Laboratory of Efficient Utilization Technology of Coal Waste Resources, Institute of Resources and Environmental Engineering, Shanxi University, No. 92 Wucheng Road, Taiyuan 030006, China; 15735175936@163.com (X.W.); 202324002003@email.sxu.edu.cn (R.D.); chenggan464@126.com (G.C.)
[2] Shanxi Laboratory of Yellow River, Shanxi University, No. 92 Wucheng Road, Taiyuan 030006, China
[3] ARC Centre of Excellence for Enabling Eco-Efficient Beneficiation of Minerals, Future Industries Institute, University of South Australia, Adelaide, SA 5095, Australia; george.abaka-wood@unisa.edu.au
* Correspondence: lienze@sxu.edu.cn

Abstract: With the advancement of large-scale coal development and utilization, low-rank coal (LRC) is increasingly gaining prominence in the energy sector. Upgrading and ash reduction are key to the clean utilization of LRC. Flotation technology based on gas/liquid/solid interfacial interactions remains an effective way to recover combustible materials and realize the clean utilization of coal. The traditional collector, kerosene, has demonstrated its inefficiency and environmental toxicity in the flotation of LRC. In this study, four eco-friendly tetrahydrofuran ester compounds (THF-series) were investigated as novel collectors to improve the flotation performance of LRC. The flotation results showed that THF-series collectors were more effective than kerosene in enhancing the LRC flotation. Among these, tetrahydrofurfuryl butyrate (THFB) exhibited the best performance, with combustible material recovery and flotation perfection factors 79.79% and 15.05% higher than those of kerosene, respectively, at a dosage of 1.2 kg/t. Characterization results indicated that THF-series collectors rapidly adsorbed onto the LRC surface via hydrogen bonding, resulting in stronger hydrophobicity and higher electronegativity. High-speed camera and particle image velocimeter (PIV) observation further demonstrated that THFB dispersed more evenly in the flotation system, reducing the lateral movement of bubbles during their ascent, lowering the impact of bubble wakes on coal particles, and promoting the stable adhesion of bubbles to the LRC surface within a shorter time (16.65 ms), thereby preventing entrainment effects. This study provides new insights and options for the green and efficient flotation of LRC.

Keywords: low-rank coal; flotation; tetrahydrofurfuryl ester

1. Introduction

The growing demand for energy has become a worldwide challenge [1]. As the most widely utilized energy source globally, coal will continue to be the preferred resource for many countries in addressing the energy crisis in the future [2–4]. However, with continuous exploitation over the past few centuries, high-quality coal has gradually been depleted, leaving large quantities of low-rank coal (LRC) available for development and utilization. In many countries, LRC has become an important industrial resource [5]. Due to the low degree of coalification, LCR has more ash and a higher volatile matter content

than other coals, such as coking coal or anthracite [6,7]. The direct combustion of LRC is not only inefficient but also causes severe environmental pollution. Therefore, recovering combustible coal from LRC is considered a promising strategy to simultaneously address environmental issues and resource challenges.

Froth flotation is the most economical and widely used technology for mineral purification [8], which can also effectively improve coal grade and reduce the risk of environmental pollution. The principle behind this technique is to separate organic carbon from gangue minerals based on the difference in their surface hydrophobicity [9–12]. However, the surface of LRC is rich in oxygen-containing functional groups, including carboxyl (-COOH), alcohol hydroxyl (-OH), and carbonyl groups (C=O) [13], resulting in strong hydrophilicity and leading to a smaller hydrophobicity difference between the coal fines and ash (primarily hydrophilic gangue minerals), thereby reducing the flotation efficiency of LRC. Therefore, the upgrading and purification of LRC using flotation technology still face numerous challenges.

Non-polar hydrocarbon oil (typically kerosene or diesel) is the most commonly used collector in the industrial coal flotation process. It primarily adsorbs onto the coal surface through hydrophobic interactions. Due to its stronger hydrophilic properties, LRC cannot effectively interact with hydrophobic hydrocarbon oils. Furthermore, hydrocarbon oil collectors exhibit low dispersion in coal flotation systems, and oil droplets tend to agglomerate easily, leading to a high consumption rate and low flotation efficiency [14]. Most notably, kerosene has characteristics such as flammability, volatility, foul odor, and poor biodegradability [15,16], posing a risk of explosion and environmental pollution during long-term use.

In order to achieve the safe, clean, and efficient flotation of LRC and reduce the use of hydrocarbon oils, one of the key factors is to develop novel green and efficient collectors [17–20]. It is well known that tetrahydrofurfuryl esters (THF) are compounds with good biodegradability and low toxicity, offering greater environmental friendliness compared to petroleum-based reagents such as kerosene. Therefore, they are regarded as potential eco-friendly alternatives. Preliminary studies have demonstrated that THF-based collectors are efficient for LRC flotation, exhibiting significantly superior flotation performance compared to dodecane [21]. However, many details about the enhancement of LRC flotation still lack clarity, including THF adsorption properties on the LRC surface, LRC surface regulation mechanisms, and the interaction mechanisms of the gas–liquid–solid phases during the flotation processing.

In this study, four tetrahydrofurfuryl ester compounds (THF-series) were selected as flotation collectors, namely tetrahydrofurfuryl acetate (THFA), tetrahydrofurfuryl propionate (THFP), tetrahydrofurfuryl butyrate (THFB), and tetrahydrofurfuryl salicylate (THFS). Flotation experiments were conducted to compare their performance with kerosene in LRC flotation, further investigating the role of THF-series collectors in LRC flotation. Additionally, various characterization techniques, including contact angle measurement, zeta potential analysis, Fourier-transform infrared spectroscopy (FTIR), X-ray photoelectron spectroscopy (XPS), total organic carbon (TOC) analysis, a high-speed camera, and particle image velocimeter (PIV), were employed to study the adsorption properties of THF-series collectors on LRC surface. The regulation mechanism of THF-series collectors on the LRC surface and the interaction among bubbles, coals, and collectors during the flotation process were explored. This study provides a more comprehensive theoretical basis for the use of THF as a novel flotation collector to improve LRC flotation efficiency and reduce environmental pollution.

2. Experimental Section

2.1. Materials

The LRC for this work was collected from an open-pit coal mine in Shanxi Province, China. The coal sample was crushed, ground, and sieved, and a fraction with a particle size of 74~106 μm was collected for subsequent use. The collectors used were kerosene and a series of tetrahydrofurfuryl esters (THF-series), including tetrahydrofurfuryl acetate (THFA, 98%), tetrahydrofurfuryl propionate (THFP, 98%), tetrahydrofurfuryl butyrate (THFB, 98%) and tetrahydrofurfuryl salicylate (THFS, 98%), all purchased from Shanghai Macklin Biochemical Co., Ltd. The molecular structures of kerosene, THFA, THFP, THFB, and THFS are shown in Figure 1. The proximate and ultimate analysis results of LRC samples before (raw coal) and after (clean coal) flotation are presented in Table 1. These results preliminarily demonstrate that flotation can effectively reduce the ash and volatile matter content of LRC and increase its carbon content, thereby achieving the purification and upgrade of LRC.
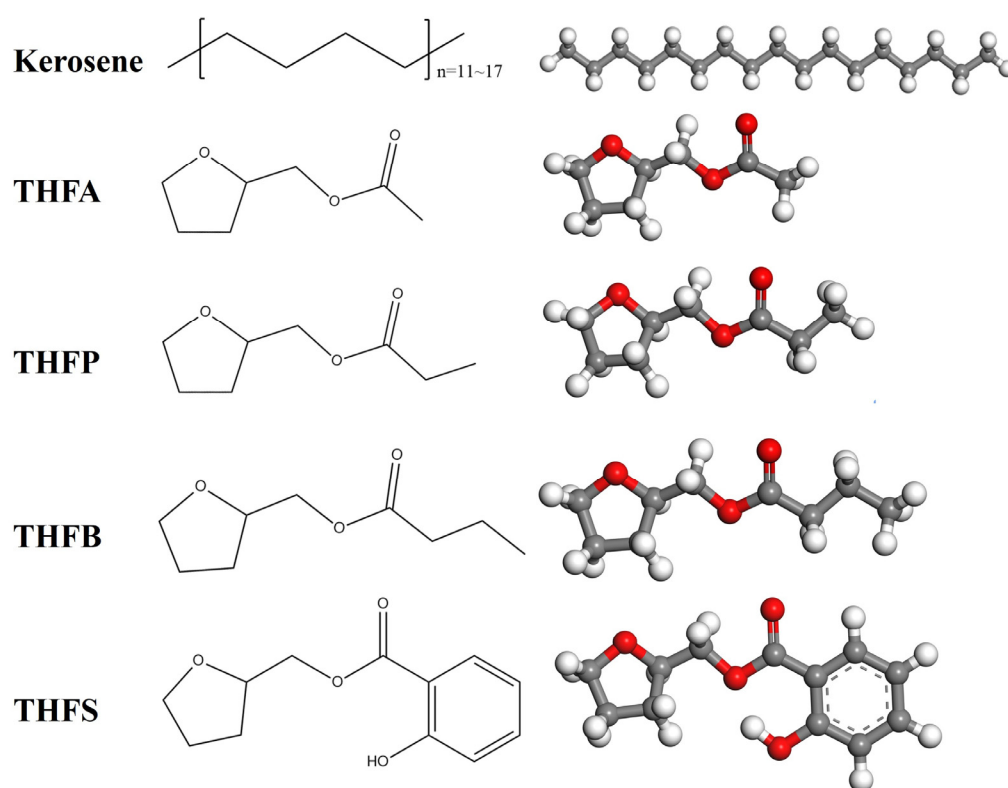

Figure 1. Molecular structure and corresponding 3D structure of collectors used in this work.

Table 1. Proximate and ultimate analysis of LRC samples before and after flotation.

Samples	Proximate Analysis (%)				Ultimate Analysis (%)				
	M_{ad}	A_{ad}	V_{ad}	FC_{ad}	C_{daf}	H_{daf}	O_{daf}	N_{daf}	S_{daf}
Raw coal	4.63	17.64	35.58	42.15	64.95	4.26	27.93	1.27	1.39
Clean coal	4.57	10.68	28.36	56.39	68.21	4.38	24.71	1.29	0.58

ad: air-dry basis; daf: dry ash-free basis; M: moisture content; A: ash content; V: volatile matter; FC: fixed carbon.

2.2. Micro-Flotation Tests

Micro-flotation experiments were conducted using a micro-flotation column as described in the previous literature [22,23]. The stirring speed and airflow rate were set to 800 rpm and 20 mL/min, respectively. First, a 5.0 g coal sample was added to a beaker and

pre-wetted for 300 s. Then, the collector (kerosene or THF-series) was added successively and conditioned for 120 s, for which the dosage of the collector relative to the mass of coal was 0.2 kg/t, 0.4 kg/t, 0.6 kg/t, 0.8 kg/t, 1.0 kg/t, and 1.2 kg/t. Finally, the mixed slurry was transferred into the flotation column with a volume of 60 mL, and then the nitrogen gas was introduced, and the froth products were collected for 180 s. During the froth flotation processing, the mixed slurry was kept stirring using a magnetic stirrer. After flotation, the clean coals and tailings were collected, filtered, dried, and weighed. The combustible material recovery (Ec) and flotation perfection factor (η_{wf}) were used to assess the flotation performance (the formulas of the two indicators can be seen in the Supporting Information (SI), as Equations (S1) and (S2)) [24]. To better demonstrate the differences in the flotation performance among various collectors, no frother was added during the flotation process. The process of wetting, pulp conditioning, and flotation is illustrated in Figure 2.
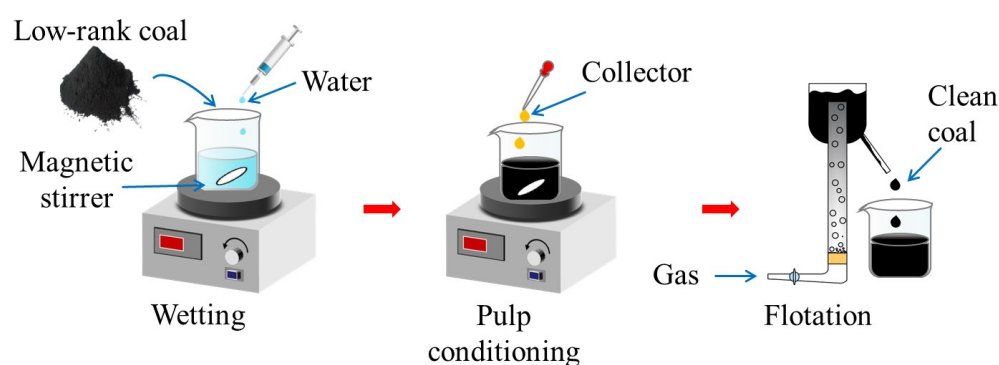

Figure 2. Schematic diagram of wetting, pulp conditioning, and flotation.

2.3. Characterizations

In this work, the contact angle was measured using a powder contact angle analysis system (DSA25B, Kress, Hamburg, Germany) through the Captive Bubble method. The FTIR study was performed using an ALPHA II (Bruker, DEU, Karlsruhe, Germany) infrared spectrometer set to a resolution of 4 cm^{-1} and scanned between 4000 cm^{-1} and 400 cm^{-1}, while the results were analyzed using Omnic software 9.2. XPS (Thermo Scientific K-Alpha, Waltham, MA, USA) was used for an accurate quantitative analysis of oxygen-containing functional groups on the coal sample surface. The coal sample surface was first scanned with a wide spectrum and then followed by a *C 1s* scan with a narrow sweep. Data processing (peak fitting) was performed with the Advantage software 6.6, and the binding was corrected based on the *C 1s* peak (284.8 eV). The TOC analysis was performed using a Vario TOC cube analyzer (Elementar Analysensysteme GmbH, Langenselbold, Hesse, Germany). The electrical properties of coal surfaces were analyzed using a ZEN3690 zeta potential instrument (Malvern, Worcestershire, UK). The interactions among bubbles, coal particles, and collectors were analyzed by using a VEO1310L high-speed camera (Phantom, Wayne, NJ, USA) and a Particle Image Velocimeter (TSI, Shoreview, MN, USA). The detailed procedures for characterizations are provided in the (Supporting Information Sections S2–S8).

3. Results and Discussion

3.1. Flotation Performances

As shown in Figure 3a,b, combustible material recovery and flotation perfection factor did not significantly increase with an increasing kerosene dosage. At a kerosene dosage of 1.2 kg/t, the maximum values of the combustible material recovery and flotation perfection factors reached only 12.51% and 3.80%, respectively, indicating that kerosene has

poor flotation performance when processing LRC. Compared to kerosene, the THF-series collectors exhibit better flotation performance for LRC. Particularly, for THFA, THFP, and THFB, combustible material recovery and flotation perfection factor sharply increased with their increasing dosage, demonstrating their excellent flotation effect for LRC. Among these, THFB performed the best, with an increase in combustible material recovery by 79.79% and flotation perfection factor by 15.05% at a dosage of 1.2 kg/t compared to kerosene. Previous studies have shown that the hydrophobicity of the LRC surface was positively correlated with the collector's adsorption and negatively correlated with the amount of oxygen-containing functional groups on the LRC surface [25,26]. This suggested that the THF-series collectors could adsorb more effectively on the LRC surface compared to kerosene and cover the hydrophilic oxygen-containing functional groups, thereby enhancing the LRC flotation performance. Further comparisons revealed that THFA, THFP, and THFB exhibited significantly better flotation performance for LRC than THFS within the THF-series collectors. The differences in their functional groups may be the primary reason for this disparity. While they all contain the tetrahydrofuran ring and ester groups, THFS also contains a benzene ring and a phenolic hydroxyl group. When THFS interacted with LRC, the benzene ring and phenolic hydroxyl group might compete with the tetrahydrofuran ring and ester group, leading to some polar groups facing outward and forming a hydrophilic layer, thereby hindering air bubble attachment to the LRC surface. However, THFA, THFP, and THFB primarily adsorb onto the coal surface by forming hydrogen bonds between their polar oxygen atoms and the oxygen-containing functional groups on the LRC surface, with their hydrocarbon chains extending outward from the coal surface [21]. Consequently, as the length of the aliphatic hydrocarbon chain increases, their flotation effectiveness improves.
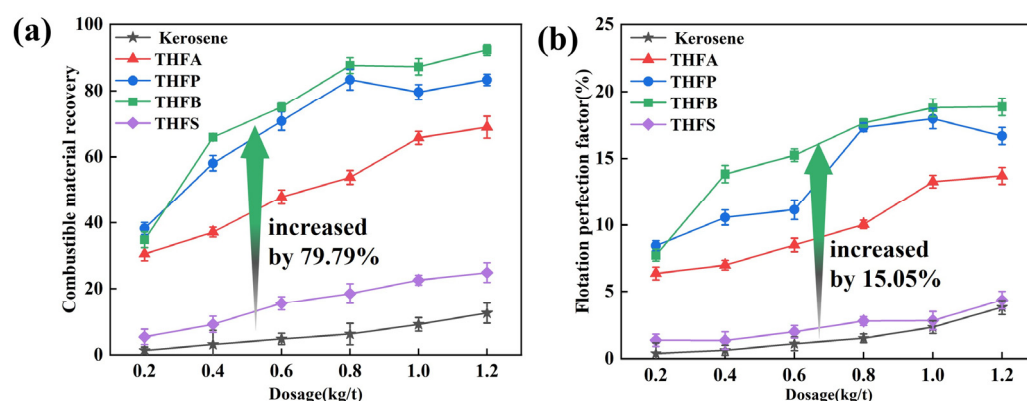

Figure 3. Flotation performances of LRC with different collectors: (**a**) combustible material recovery; (**b**) flotation perfection factor.

3.2. Adsorption Property Analysis

The flotation experiment results indicate that the THF-series collectors improve LRC floatability by achieving better adsorption on the LRC surface. Previous studies have shown that changes in the total organic carbon (TOC) of flotation pulp before and after reagent treatment can also reflect the adsorption capacity of reagents on the mineral surface [27]. Therefore, this study further investigated the adsorption characteristics of LRC with different collectors by examining the variation of q_{TOC} (the calculation method could be seen in Supporting Information (Equations (S3) and (S4))) over time. As shown in Figure 4, the adsorption capacity of LRC for different collectors increased initially with time before attaining equilibrium, which varied with the collector type. Compared to kerosene, THF-series collectors adsorbed more rapidly onto the LRC surface, with THFA, THFP, and THFB reaching adsorption equilibrium within 60 s, THFS reaching

equilibrium within 80 s, and kerosene requiring 120 s to achieve equilibrium. Furthermore, the maximum adsorption capacity of LRC for THF-series collectors was also superior to that of kerosene, with THFB exhibiting the best adsorption performance, achieving a maximum adsorption capacity 6.7 times higher than that of kerosene. This finding further confirms that THF-series collectors adsorb more effectively onto the LRC surface, enhancing its flotation efficiency.
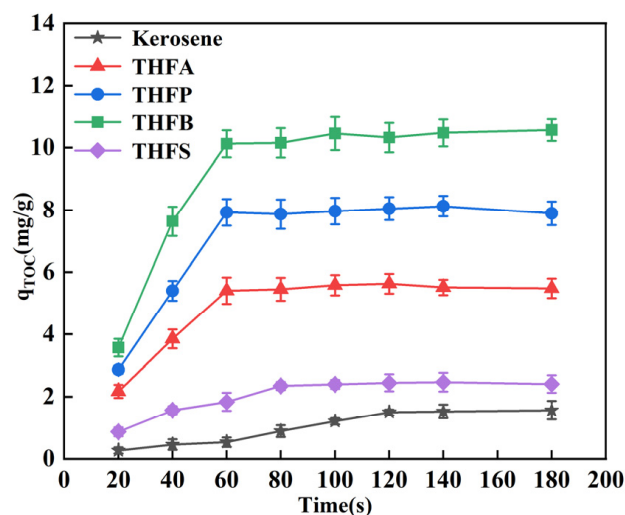

Figure 4. Adsorption capacity of different collectors on the LRC surface over time.

FTIR was employed to further analyze the adsorption characteristics of the collectors on the LRC surface. As shown in Figure 5a, these absorption peaks at 3689.74 cm^{-1}, 3620.79 cm^{-1}, 3442.68 cm^{-1}, 3438.58 cm^{-1}, 3436.11 cm^{-1}, 3432.01 cm^{-1}, and 3429.55 cm^{-1} indicate the presence of free hydroxyl (-OH) and hydroxyl groups (-OH) from alcohols and phenols on the LRC surface, respectively [28,29]. Additionally, the peaks at 2921.48 cm^{-1} and 2856.63 cm^{-1} are attributed to the symmetric and antisymmetric stretching vibrations of -CH$_2$/-CH$_3$ groups [30,31]. Moreover, the peak at 1600 cm^{-1} corresponds to the stretching vibration of the carbonyl group (-C=O) [19]. The peaks at 1027.09 cm^{-1} represent the stretching vibration of the -C-O group [32], while the characteristic peak of kaolinite appears at 913 cm^{-1} [33]. This indicates that the LRC is rich in oxygen-containing functional groups and hydrophilic gangue minerals, which are unfavorable for the adsorption of kerosene but facilitate the formation of hydrogen bonds with THF-series collectors. Further analysis of Figure 5a reveals the appearance of a new peak at 3024.08 cm^{-1} on the LRC surface after treatment with THF-series collectors corresponding to the ring -CH$_2$ symmetric stretching. This indicates that THF-series collectors are effectively adsorbed onto the LRC surface. Additionally, after the adsorption of THF-series collectors, the intensities of the -OH peaks (3689.74 cm^{-1} and 3620.79 cm^{-1}), -C=O peak (1600 cm^{-1}), -C-O peak (1027.09 cm^{-1}), and kaolinite peak (913 cm^{-1}) all decreased, suggesting that THF-series collectors can effectively shield the hydrophilic sites of the LRC surface, increasing its hydrophobicity. Moreover, a significant shift in the hydroxyl (-OH) stretching peak at 3429.55 cm^{-1} was observed on the LRC surface after treatment with THF-series collectors. Specifically, the peak at 3429.55 cm^{-1} (raw LRC) was shifted to 3432.01 cm^{-1} (LRC treated with THFA), 3442.68 cm^{-1} (LRC treated with THFP), 3438.58 cm^{-1} (LRC treated with THFB), and 3436.61 cm^{-1} (LRC treated with THFS). This phenomenon further confirms the formation of hydrogen bonds between THF-series collectors and the hydroxyl (-OH) groups on the LRC surface [34].
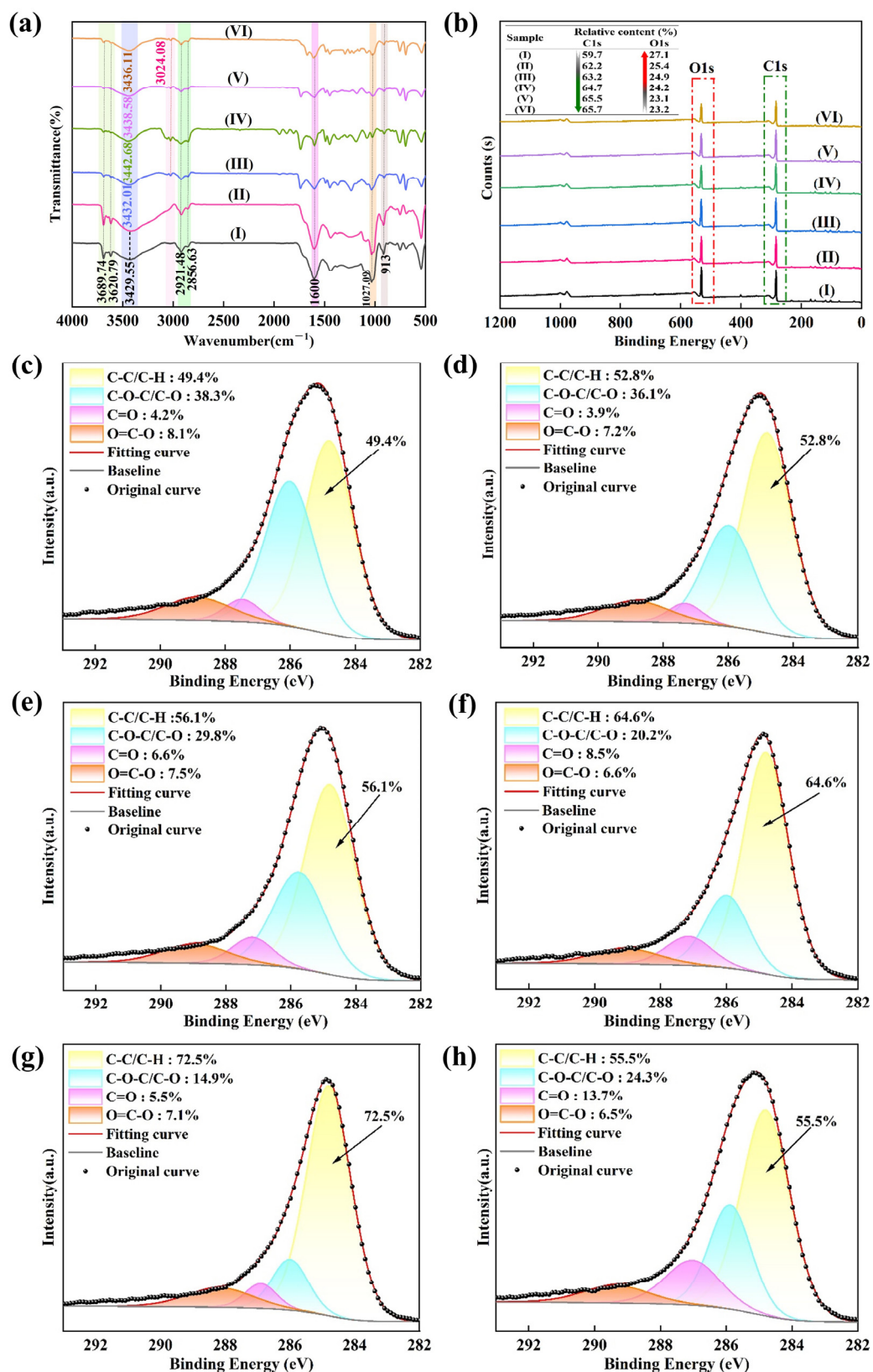
Figure 5. (**a**) FTIR spectra and (**b**) XPS survey of different samples ((I) LRC and LRC treated with (II) kerosene, (III) THFA, (IV) THFP, (V) THFB, and (VI) THFS); (**c–h**) *C 1s* peaks of different samples ((**c**) LRC and LRC treated with (**d**) kerosene, (**e**) THFA, (**f**) THFP, (**g**) THFB, and (**h**) THFS).

The changes in the surface elemental composition and functional groups of LRC before and after the adsorption of different collectors were further analyzed using XPS,

and the results are presented in Figure 5b–h. As shown in Figure 5b, C (285 eV) and O (532 eV) [28,29] were the primary elements on the LRC surface. Upon the adsorption of the collectors, the C elemental content on the LRC surface increased, while the O elemental content decreased. This was because the adsorption of the collectors effectively masked the oxygen-containing sites on the LRC surface [35]. After treatment with THFA, THFP, THFB, and THFS, the O content on the LRC surface decreased by 2.2%, 2.9%, 4.0%, and 3.9%, respectively, while the C content increased by 3.5%, 5.0%, 5.8%, and 6.0%, respectively. These results indicated that the THF-series collectors have better adsorption efficiency, masking more oxygen-containing functional groups contained on the LRC surface. The higher C content and lower O content suggested that the modified LRC surface was more hydrophobic than the raw LRC surface [36]. Figure 5c–h further illustrate the *C 1s* peaks on the LRC surface before and after treatment with different collectors. The binding energies of 284.8 eV, 286.0 eV, 287.2 eV, and 289.1 eV correspond to C-C/C-H, C-O-C/C-O, C=O, and O=C-O, respectively [37–40]. These results indicate the presence of C-C/C-H, C-O-C/C-O, C=O, and O=C-O groups on the LRC surface. The C-O-C/C-O, C=O, and O=C-O groups exhibit strong hydrophilic properties, whereas the C-C/C-H groups are hydrophobic. Previous studies have shown that the higher the content of oxygen-containing functional groups on the LRC surface, the greater its hydrophilicity and the lower its floatability [36]. By comparing Figure 5c,d, it is observed that after treatment with kerosene, the content of hydrophobic groups (C-H/C-C) on the LRC surface slightly increased from 49.4% to 52.8%. Meanwhile, the content of hydrophilic groups C-O-C/C-O, C=O, and O=C-O decreased from 38.3%, 4.2%, and 8.1% to 36.1%, 3.9%, and 7.2%, respectively. This suggests that the adsorption of kerosene on the LRC surface is limited. In comparison, the THF-series collectors significantly increased the proportion of hydrophobic groups (C-H/C-C) on the LRC surface and reduced the overall proportion of hydrophilic groups (C-O-C/C-O, C=O, and O=C-O), indicating that the THF-series collectors exhibit stronger adsorption on the LRC surface than kerosene, which is advantageous for flotation. Further analysis revealed that among the THF-series collectors, the increase in the content of hydrophobic groups (C-H/C-C) on the LRC surface follows the order of THFB (23.1%) > THFP (15.2%) > THFA (6.7%) > THFS (6.1%). This result further corroborates the findings from the flotation experiments. Additionally, among the three types of hydrophilic groups (C-O-C/C-O, C=O, and O=C-O), the most significant reduction in content was observed for the C-O-C/C-O groups after interaction with the THF-series collectors. This suggests that among the hydrophilic groups, the C-O-C/C-O groups are primarily involved in forming hydrogen bonds with the THF-series collectors, which is consistent with previous research [24].

3.3. Changes in LRC Surface Properties

The interaction between different collectors and LRC during the flotation process was further investigated by analyzing the changes in the surface properties of LRC before and after the action of collectors. First, the changes in LRC surface wettability were examined by measuring the contact angle of bubbles on the LRC surface before and after the action of collectors. As illustrated in Figure 6a, the contact angle of LRC without a collector is 34.4°, indicating that the LRC has strong hydrophilicity, which is unfavorable for its flotation upgrading. After the addition of kerosene and THF-series collectors, the contact angle increased in all cases. The primary reason for this phenomenon is that both kerosene and THF-series collectors can cover the surface of LRC, increasing its hydrophobicity and raising the contact angle. However, after treatment with kerosene, the contact angle of LRC only increased slightly from 34.4° to 35.6°, suggesting that the adsorption of kerosene on the LRC surface is minimal. In comparison, the contact angle of LRC increased significantly after the application of THF-series collectors, with THFB exhibiting the most

pronounced effect, achieving an increase of 49.3°. This result suggests that the THF-series collectors can effectively adsorb onto the LRC surface, significantly reducing its wettability. This is because kerosene primarily adsorbs on the LRC surface through hydrophobic interactions and van der Waals forces, whereas THF-series collectors interact with LRC mainly through hydrogen bonding. The abundance of oxygen-containing functional groups on the LRC surface makes THF-series collectors more effective in adsorbing onto its surface than kerosene.
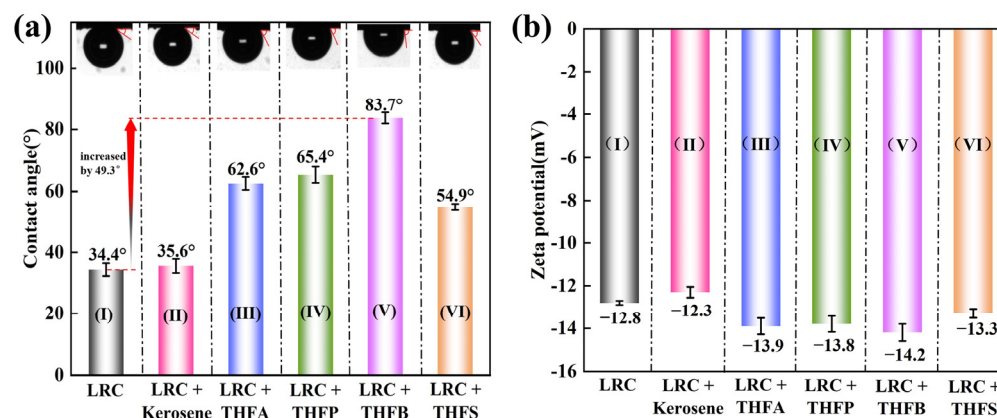
Figure 6. Changes in LRC surface (**a**) wettability and (**b**) electrical properties before and after actions of different collectors ((I) LRC and LRC treated with (II) kerosene, (III) THFA, (IV) THFP, (V) THFB, and (VI) THFS).

Further studies were conducted on the electrical properties of the LRC surface. As shown in Figure 6b, under the experimental conditions, the surface potential of LRC is negative in the absence of any collector, which is consistent with the findings of previous studies [41]. Upon the addition of kerosene, the zeta potential of the LRC surface only slightly increased, rising from −12.8 mV to −12.3 mV. It was found that non-polar collectors like kerosene adsorb onto the coal surface via hydrophobic interactions, with their non-polar molecules covering the hydrophilic groups on the coal surface, thereby reducing the negative charge on the coal particle surface and increasing the zeta potential [42]. However, due to the weaker adsorption capacity of kerosene on the surface of LRC, the increase in surface potential was minimal. After the addition of THF-series collectors, the zeta potential of the LRC surface decreased, with a more pronounced change compared to kerosene. On the one hand, the polar groups in THF-series collectors can form hydrogen bonds with oxygen-containing groups on the LRC surface, increasing the surface electronegativity and thus lowering the zeta potential [43]. On the other hand, differences in the adsorption amounts of the collectors on the LRC surface also led to variations in the extent of surface potential change. The greater the adsorption amount, the larger the change in surface potential. Consequently, in this study, the impact of the collectors on the zeta potential of the LRC surface followed the trend of THFB > THFP > THFA > THFS > kerosene, which is generally consistent with the flotation test results.

3.4. The Role of Bubbles in LRC Flotation

A further investigation was conducted using THFB, the most effective collector from the THF-series, and kerosene. The study focused on bubble behavior in collector solutions and their interactions with LRC. Figure 7a presents the flow field in the wake region of bubbles in different collector solutions. The color map represents velocity ranges [44] from 0.005 m/s (blue) to 0.56 m/s (red). Further analysis revealed that the velocity distributions in Figure 7(aI,aII) are very similar, particularly within the *Y*-axis range of 50~70 mm, where a distinct red region is observed, indicating the highest velocity. In comparison, the red region

in Figure 7(aIII) within the same *Y*-axis range appears broader, which may imply a more uniform velocity distribution or more intense mixing in this area. The density of streamlines reflects variations in fluid velocity gradients under different conditions. Among the three cases, the streamlines in Figure 7(aIII) exhibit the most uniform distribution, indicating the highest and most homogeneous mixing efficiency of the fluid within the container. This suggests that THFB disperses more uniformly in the flotation system compared to kerosene, increasing the collision probability with LRC particles and demonstrating superior adsorption performance. Additionally, the direction of the streamlines can be used to infer the rising path of bubbles. In all three images, the streamlines show an upward trend along the *Y*-axis, which is consistent with the bubble trajectories shown in Figure 7b. The distribution of streamlines along the *X*-axis reveals the lateral displacement or rotation of bubbles during their ascent. Combined with Figure 7b, it can be deduced that bubbles in the THFB solution exhibit smaller lateral deviations, which prevents LRC particles in the flotation system from passing through the wake region. Consequently, the particles are not affected by bubble wakes, avoiding entrainment and achieving flotation [45].
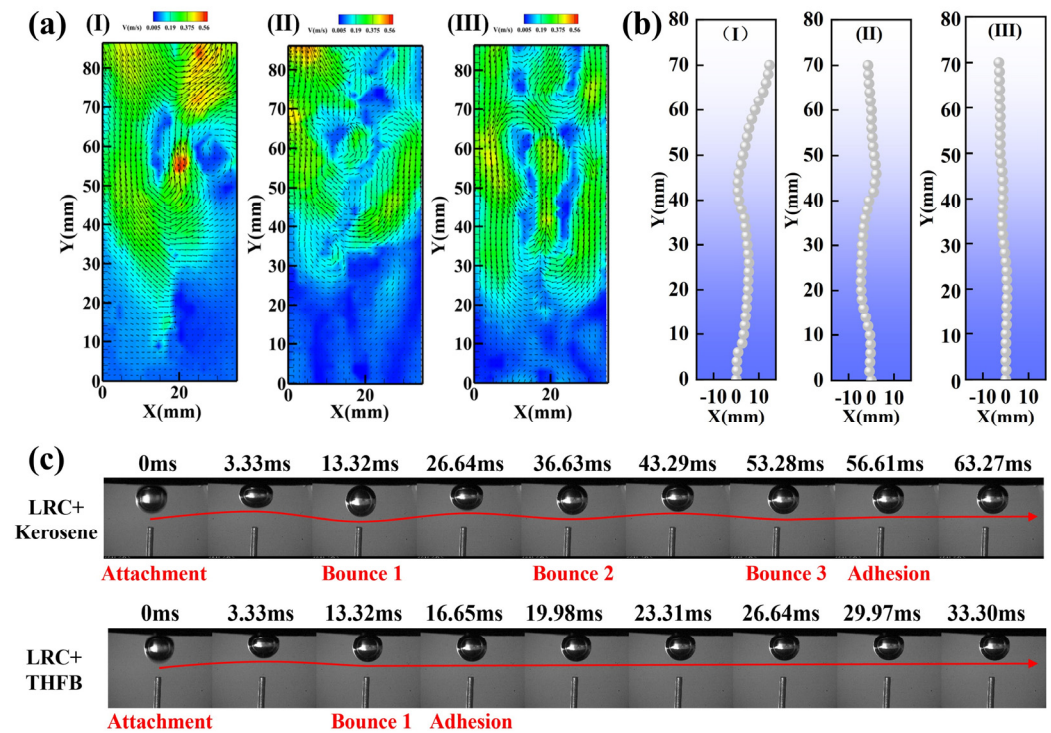

Figure 7. (**a**) Flow field of bubble trailing vortex region and (**b**) bubble motion trajectory in different collector solutions ((**I**) deionized water, (**II**) kerosene solution, (**III**) THFB solution); (**c**) snapshots of a bubble attachment and adhesion on the LRC surface (after kerosene or THFB treatment) captured by a high-speed camera.

Figure 7c shows the details of the bubble-impinging LRC surface treated with kerosene or THFB recorded using a high-speed camera. For kerosene, the impinging bubble bounces three times on the LRC surface before finally adhering at 56.61 ms. However, only one slight bounce happens for the THFB-treated LRC, and the adhesion occurs at 16.65 ms. This demonstrates that the use of the THFB collector can induce much stronger interfacial interaction between the bubble and the LRC surface in the water system. Consequently, the bubble adheres to the LRC surface more quickly and stably, enhancing the flotation performance of the LRC.

4. Conclusions

This study selected four efficient and eco-friendly tetrahydrofuran ester (THF-series) collectors to improve the flotation efficiency of LRC. Through flotation experiments, the flotation performance of THF-series collectors was compared with that of kerosene. Various characterization methods were used to investigate the adsorption properties and regulation mechanisms of THF-series on the LRC surface. High-speed imaging and PIV were also employed to analyze the interactions between the gas, liquid, and solid phases during the flotation process. The main conclusions of this study are as follows:

(1) THF-series collectors exhibited superior flotation performance for LRC. Among them, THFB demonstrated the best effect, with combustible material recovery 79.79% higher than that of kerosene and a flotation perfection factor that increased by 15.05% at a dosage of 1.2 kg/t.

(2) THF-series collectors can adsorb more quickly and efficiently onto the LRC surface to enhance its floatability. In this study, THFB reached adsorption equilibrium within 60 s, with a maximum adsorption capacity of 6.7 times that of kerosene. The THF-series collectors primarily interact with LRC through hydrogen bonding. After adsorption, THF-series collectors effectively mask the oxygen-containing sites on the LRC surface, reducing its wettability and enhancing its electronegativity.

(3) THFB collectors can disperse more uniformly in the flotation system, reducing the lateral movement of bubbles during their ascent, decreasing the influence of bubble wakes on coal particles, and preventing entrainment effects. After treatment with THFB, bubbles could stably adhere to the LRC surface within 16.65 ms, significantly improving the flotation efficiency of LRC.

References

1. Zheng, K.; Zhang, W.; Li, Y.; Ping, A.; Wu, F.; Xie, G.; Xia, W. Enhancing flotation removal of unburned carbon from fly ash by coal tar-based collector: Experiment and simulation. *Fuel* **2023**, *332*, 126023. [CrossRef]
2. Kang, W.; Ma, Z. Pyhsical and chemical properties of coal pyrite and flotation desulfurization. *Clean Coal Technol.* **2022**, *28*, 109–117.

3. Karamaneas, A.; Koasidis, K.; Frilingou, N.; Xexakis, G.; Nikas, A.; Doukas, H. A stakeholder-informed modelling study of Greece's energy transition amidst an energy crisis: The role of natural gas and climate ambition. *Renew. Sustain. Energy Transit.* **2023**, *3*, 100049. [CrossRef]

4. Cheng, G.; Li, Y.; Cao, Y.; Wang, X.; Li, E.; Guo, Y.; Lau, E.V. New Insights on the Understanding of Sulfur-Containing Coal Flotation Desulfurization. *Minerals* **2024**, *14*, 981. [CrossRef]

5. Liao, Y.; Yang, Z.; An, M.; Ma, L.; Yang, A.; Cao, Y.; Chen, L.; Ren, H. Alkanes-esters mixed collector enhanced low rank coal flotation: Interfacial interaction between oil drop and coal particle. *Fuel* **2022**, *321*, 124045. [CrossRef]

6. Xia, Y.; Xing, Y.; Gui, X. Oily collector pre-dispersion for enhanced surface adsorption during fine low-rank coal flotation. *J. Ind. Eng. Chem.* **2020**, *82*, 303–308. [CrossRef]

7. Nyashina, G.S.; Kuznetsov, G.V.; Strizhak, P.A. Energy efficiency and environmental aspects of the combustion of coal-water slurries with and without petrochemicals. *J. Clean. Prod.* **2018**, *172*, 1730–1738. [CrossRef]

8. Lu, Y.; Liu, W.; Wang, X.; Cheng, H.; Cheng, F.; Miller, J.D. Lauryl phosphate flotation chemistry in barite flotation. *Minerals* **2020**, *10*, 280. [CrossRef]

9. Chen, S.; Tang, L.; Tao, X.; Chen, L.; Yang, Z.; Li, L. Effect of oxidation processing on the surface properties and floatability of Meizhiyou long-flame coal. *Fuel* **2017**, *210*, 177–186. [CrossRef]

10. Chen, S.; Yang, Z.; Chen, L.; Tao, X.; Tang, L.; He, H. Wetting thermodynamics of low rank coal and attachment in flotation. *Fuel* **2017**, *207*, 214–225. [CrossRef]

11. Chen, S.; Tao, X.; Wang, S.; Tang, L.; Liu, Q.; Li, L. Comparison of air and oily bubbles flotation kinetics of long-flame coal. *Fuel* **2019**, *236*, 636–642. [CrossRef]

12. Huang, Y.; Takaoka, M.; Takeda, N.; Oshita, K. Partial removal of PCDD/Fs, coplanar PCBs, and PCBs from municipal solid waste incineration fly ash by a column flotation process. *Environ. Sci. Technol.* **2007**, *41*, 257–262. [CrossRef] [PubMed]

13. Wen, B.; Xia, W.; Sokolovic, J.M. Recent advances in effective collectors for enhancing the flotation of low rank/oxidized coals. *Powder Technol.* **2017**, *319*, 1–11. [CrossRef]

14. Chen, S.; Tang, L.; Tao, X.; He, H.; Chen, L.; Yang, Z. Enhancing flotation performance of low rank coal by improving its hydrophobicity and the property of oily bubbles using 2-ethylhexanol. *Int. J. Miner. Process.* **2017**, *167*, 61–67. [CrossRef]

15. Lam, N.L.; Chen, Y.; Weyant, C.; Venkataraman, C.; Sadavarte, P.; Johnson, M.A.; Smith, K.R.; Brem, B.T.; Arineitwe, J.; Ellis, J.E. Household light makes global heat: High black carbon emissions from kerosene wick lamps. *Environ. Sci. Technol.* **2012**, *46*, 13531–13538. [CrossRef] [PubMed]

16. Li, E.; Xiao, X.; Wang, X.; Pan, Z.; Qin, Y.; Gao, G.; Du, Z.; Cheng, F. Interfacial interaction of emulsion collector in enhancing low-rank coal flotation. *Colloids Surf. A Physicochem. Eng. Asp.* **2024**, *692*, 133965. [CrossRef]

17. Xia, Y.; Yang, Z.; Zhang, R.; Xing, Y.; Gui, X. Performance of used lubricating oil as flotation collector for the recovery of clean low-rank coal. *Fuel* **2019**, *239*, 717–725. [CrossRef]

18. Li, M.; Xia, Y.; Zhang, Y.; Ding, S.; Rong, G.; Cao, Y.; Xing, Y.; Gui, X. Mechanism of shale oil as an effective collector for oxidized coal flotation: From bubble–particle attachment and detachment point of view. *Fuel* **2019**, *255*, 115885. [CrossRef]

19. Xia, W.; Ni, C.; Xie, G. Effective flotation of lignite using a mixture of dodecane and 4-dodecylphenol (DDP) as a collector. *Int. J. Coal Prep. Util.* **2016**, *36*, 262–271. [CrossRef]

20. Xing, Y.; Gui, X.; Cao, Y.; Wang, D.; Zhang, H. Clean low-rank-coal purification technique combining cyclonic-static microbubble flotation column with collector emulsification. *J. Clean. Prod.* **2017**, *153*, 657–672. [CrossRef]

21. Jia, R.; Harris, G.H.; Fuerstenau, D.W. An improved class of universal collectors for the flotation of oxidized and/or low-rank coal. *Int. J. Miner. Process.* **2000**, *58*, 99–118. [CrossRef]

22. Hancer, M.; Celik, M.; Miller, J.D. The significance of interfacial water structure in soluble salt flotation systems. *J. Colloid Interface Sci.* **2001**, *235*, 150–161. [CrossRef] [PubMed]

23. Li, E.; Zhang, Y.; Du, Z.; Li, D.; Cheng, F. Bubbles facilitate ODA adsorption and improve flotation recovery at low temperature during KCl flotation. *Chem. Eng. Res. Des.* **2017**, *117*, 557–563. [CrossRef]

24. Hu, X.; Li, Y.; Li, W. Recycling of waste plastic combustion soot and diesel oil mixing to prepare a new collector to improve the performance of low-rank coal flotation. *Powder Technol.* **2024**, *439*, 119727. [CrossRef]

25. Cheng, G.; Li, Z.; Ma, Z.; Cao, Y.; Sun, L.; Jiang, Z. Optimization of collector and its action mechanism in lignite flotation. *Powder Technol.* **2019**, *345*, 182–189. [CrossRef]

26. He, J.; Liu, C.; Yao, Y. Flotation intensification of the coal slime using a new compound collector and the interaction mechanism between the reagent and coal surface. *Powder Technol.* **2018**, *325*, 333–339. [CrossRef]

27. Ge, W.; Liu, J.; Ren, H.; Zhu, Y.; Han, W.; Han, Y. Enhanced mixed flotation of copper–molybdenum ore using dodecyl dimethyl betaine-emulsified kerosene as environmentally friendly collector. *J. Clean. Prod.* **2024**, *447*, 141576. [CrossRef]

28. Lyu, X.; You, X.; He, M.; Zhang, W.; Wei, H.; Li, L.; He, Q. Adsorption and molecular dynamics simulations of nonionic surfactant on the low rank coal surface. *Fuel* **2018**, *211*, 529–534. [CrossRef]

29. Li, Y.; Xia, W.; Peng, Y.; Xie, G. A novel coal tar-based collector for effective flotation cleaning of low rank coal. *J. Clean. Prod.* **2020**, *273*, 123172. [CrossRef]

30. Ban, Y.; Jin, L.; Zhu, J.; Liu, F.; Hu, H. Insights into effect of $Ca(OH)_2$ on pyrolysis behaviors and products distribution of Hongshaquan coal. *Fuel* **2022**, *307*, 121791. [CrossRef]

31. Zhu, X.-n.; Wang, D.-z.; Ni, Y.; Wang, J.-x.; Nie, C.-c.; Yang, C.; Lyu, X.-j.; Qiu, J.; Li, L. Cleaner approach to fine coal flotation by renewable collectors prepared by waste oil transesterification. *J. Clean. Prod.* **2020**, *252*, 119822. [CrossRef]

32. Xu, M.; Xing, Y.; Cao, Y.; Gui, X. Waste colza oil used as renewable collector for low rank coal flotation. *Powder Technol.* **2019**, *344*, 611–616. [CrossRef]

33. Wang, S.; Liu, K.; Ma, X.; Tao, X. Comparison of flotation performances of low-rank coal with lower ash content using air and oily bubbles. *Powder Technol.* **2020**, *374*, 443–448. [CrossRef]

34. Wang, C.; Xing, Y.; Xia, Y.; Zhang, R.; Wang, S.; Shi, K.; Tan, J.; Gui, X. Investigation of interactions between oxygen-containing groups and water molecules on coal surfaces using density functional theory. *Fuel* **2021**, *287*, 119556. [CrossRef]

35. Zhou, G.; Xu, C.; Cheng, W.; Zhang, Q.; Nie, W. Effects of oxygen element and oxygen-containing functional groups on surface wettability of coal dust with various metamorphic degrees based on XPS experiment. *J. Anal. Methods Chem.* **2015**, *2015*, 467242. [CrossRef]

36. Wan, H.; Hu, X.; Luukkanen, S.; Qu, J.; Zhang, C.; Xue, J.; Li, H.; Yang, W.; Yang, S.; Bu, X. Effect of the oxygen-containing functional group on the adsorption of hydrocarbon oily collectors on coal surfaces. *Physicochem. Probl. Miner. Process.* **2022**, *58*, 149937. [CrossRef]

37. Grzybek, T.; Pietrzak, R.; Wachowska, H. X-ray photoelectron spectroscopy study of oxidized coals with different sulphur content. *Fuel Process. Technol.* **2002**, *77*, 1–7. [CrossRef]

38. Pietrzak, R.; Wachowska, H. The influence of oxidation with HNO_3 on the surface composition of high-sulphur coals: XPS study. *Fuel Process. Technol.* **2006**, *87*, 1021–1029. [CrossRef]

39. Xia, Y.; Yang, Z.; Zhang, R.; Xing, Y.; Gui, X. Enhancement of the surface hydrophobicity of low-rank coal by adsorbing DTAB: An experimental and molecular dynamics simulation study. *Fuel* **2019**, *239*, 145–152. [CrossRef]

40. Xia, W.; Niu, C.; Li, Y. Effect of heating process on the wettability of fine coals of various ranks. *Can. J. Chem. Eng.* **2017**, *95*, 475–478. [CrossRef]

41. Li, Y.; Xia, W.; Pan, L.; Tian, F.; Peng, Y.; Xie, G.; Li, Y. Flotation of low-rank coal using sodium oleate and sodium hexametaphosphate. *J. Clean. Prod.* **2020**, *261*, 121216. [CrossRef]

42. Ji, D.G.; Cai, Y.H.; Guo, X.L.; Peng, S.Q.; Wei, S.G. Research of Optimize Performance of Coal Flotation Collectors. *Adv. Mater. Res.* **2012**, *361*, 296–300. [CrossRef]

43. Gui, X.; Xing, Y.; Wang, T.; Cao, Y.; Miao, Z.; Xu, M. Intensification mechanism of oxidized coal flotation by using oxygen-containing collector α-furanacrylic acid. *Powder Technol.* **2017**, *305*, 109–116. [CrossRef]

44. Pan, G.; Zhu, H.; Shi, Q.; Zhang, Y.; Zhu, J.; Ou, Z.; Gao, L. Effect of bubble trailing vortex on coal slime motion in flotation. *Fuel* **2023**, *334*, 126802. [CrossRef]

45. Shi, Q.; Zhu, H.; Shen, T.; Qin, Z.; Zhu, J.; Gao, L.; Ou, Z.; Zhang, Y.; Pan, G. Effect of frother on bubble entraining particles in coal flotation. *Energy* **2024**, *288*, 129711. [CrossRef]

46. Lu, Y.; Li, E.; Cheng, H.; Wang, X.; Du, Z.; Cheng, F.; Miller, J.D. Effect of oxygen functional groups on the surface properties and flotation response of fine coal, comparison of rank with oxidation. *Int. J. Coal Prep. Util.* **2018**, *41*, 290–306. [CrossRef]